DTU Library

All dielectric self-induced back-action trapping.

Gøtzsche, Benjamin Falkenberg; Kristensen, Philip Trøst; Wubs, Martijn

Published in:
Proceedings of SPIE

Link to article, DOI:
10.1117/12.3027439

Publication date:
2024

Document Version
Publisher's PDF, also known as Version of record

All dielectric self-induced back-action trapping

Benjamin Falkenberg Gøtzsche[a,b], Philip Trøst Kristensen[a,b], and Martijn Wubs[a,b]

[a]Department of Electrical and Photonics Engineering, Technical University of Denmark, Building 345, 2800 Kgs. Lyngby, Denmark
[b]NanoPhoton - Center for Nanophotonics, Ørsteds Plads 345A, 2800 Kgs. Lyngby, Denmark

Abstract

Strong field gradients in electromagnetic resonators can trap individual nanospheres. Moreover, the presence of the sphere in the resonator can give rise to self-induced back-action (SIBA), which increases the trap stiffness beyond standard dipolar force theory. In this work, we investigate SIBA in a system with a silica sphere of 16 nm in diameter in a dielectric nanocavity with a strongly localized electric field. We analyze the optical forces in a novel framework based on perturbation theory with quasi-normal modes, where modifications to the gradient and scattering forces are found to arise due to the presence of the particle, thus capturing the back-action effect. This gives closed-form expressions with clear insight into the mechanism of SIBA, and provides an efficient method of estimating optical forces when SIBA is present. We compare the results with reference calculations based on the Maxwell Stress Tensor formalism and find good agreement.

Keywords: Optical trapping, nanophotonics, dielectrics, self-induced backaction, near-field optics, non-Hermitian physics

Introduction

Within the last few decades, optical trapping has gained significant scientific interest. This interest stems from the seminal work on the optical tweezer, pioneered by Arthur Ashkin [1], whereby focusing a free-space laser using a lens with high numerical aperture allowed fixation and control of a single glass sphere of a few μm in diameter in an aqueous environment. The focal point of the free-space laser is subject to the diffraction limit, and thus, exhibits unfavorable power requirements when the dimensions of the trapped sphere approach the nanometer scale. The emergent field of nanoplasmonics offers the ability to manipulate light below the diffraction limit, whereby optical trapping of single proteins using metallic nanostructures has become feasible [2]. With recent advances in the design and fabrication process of dielectric material [3], dielectric nanocavities have similarly shown field confinement below the diffraction limit manifesting themselves as promising platforms for optically trapping with near-zero loss, complementing the more lossy plasmonic trapping.
In trapping experiments using dielectric nanostructures, SIBA has been demonstrated [4, 5], increasing the optical force beyond the prediction of dipolar optical force theory. The mechanism of SIBA is generally attributed to a frequency shift of the electromagnetic resonator due to the particle presence [6] but is for practical calculations typically calculated using the Maxwell Stress Tensor (MST) formalism. While the MST formalism is of general validity, analytical results are generally difficult to obtain for complex resonator geometries, and one therefore resorts to numerical simulations, which hinders analysis of the physical mechanisms responsible for the effect. In this work, we model the intra-cavity field using the quasi-normal mode (QNM) formalism [7], thus taking non-Hermitian physics of the electromagnetic resonator into account, and using perturbation theory in the QNMs, we find corrections to standard dipolar force theory. Comparing to independent reference calculations using the MST formalism, we show that these corrections are important for a single-moded dielectric nanocavity when hosting a silica sphere of 16 nm in diameter, and attribute this to SIBA.

Optical Trapping and Optical Micromanipulation XXI, edited by Kishan Dholakia, Halina Rubinsztein-Dunlop, Giovanni Volpe, Proc. of SPIE Vol. 13112, 1311203
 · doi: 10.1117/12.3027439

Method

For a spherical particle with radius r_{sph} much smaller than the wavelength of the incident electromagnetic field, we may appropriately model the sphere as a dipole, and calculate the cycle-averaged force acting on the dipole as [8],

$$\langle \mathbf{F} \rangle = \frac{\alpha_{\mathrm{R}}}{4} \nabla(|\mathbf{E}|^2) + \frac{\sigma}{\mathrm{c}} \langle \mathbf{S} \rangle + \mathrm{c}\sigma \left[\nabla \times \langle \mathbf{L} \rangle \right], \tag{1}$$

where $\mathbf{E}$ is the phasor of a harmonic incident field of the form $\mathbf{E}(\mathbf{r},t) = \mathrm{Re}\{\mathbf{E}(\mathbf{r})\exp(-\mathrm{i}\omega t)\}$ where ω is the angular frequency of light, $\langle\cdot\rangle$ denotes cycle-averaging, $\langle \mathbf{S} \rangle$ and $\langle \mathbf{L} \rangle$ are the cycle-averaged Poynting vector and the transverse spin density of the electric field, respectively, c the speed of light, ϵ_0 the vacuum permittivity, and $\sigma = \alpha_{\mathrm{I}} k_0/\epsilon_0$ is the absorption cross-section, where k_0 is the free-space wave number. α_{R} and α_{I} are the real and imaginary parts of the polarizability $\alpha(\omega) = \alpha_0 / \left[1 - \mathrm{i}\frac{k_0^3}{6\pi\epsilon_0}\alpha_0\right]$, respectively, with $\alpha_0 = 4\pi\epsilon_0 r_{\mathrm{sph}}^3(\epsilon_{\mathrm{p}} - 1)/(\epsilon_{\mathrm{p}} + 2)$, where ϵ_{p} is the relative permittivity of the sphere.

Inherent in the use of Eq. (1) is the assumption that the electromagnetic field is unaltered by the presence of the particle. In order to derive a semi-analytical description for the trapping of the nanosphere using the intra-cavity field of a dielectric nanocavity, we expand $\mathbf{E}(\mathbf{r})$ using QNMs.

QNMs are discrete solutions to the wave equations, subject to a radiation condition [7]. The radiation condition turns the wave equation into a non-Hermitian eigenvalue problem, where the μ-th eigenmode has a complex eigenvalue of the form $\tilde{\omega}_\mu = \omega_\mu - \mathrm{i}\gamma_\mu$ where ω_μ is the (angular) resonance frequency and γ_μ the field escape rate, from which the quality factor of the μ-th mode may be immediately extracted as $Q_\mu = \omega_\mu/(2\gamma_\mu)$. Due to the dissipative nature of the QNMs, the fields are spatially divergent, and are normalized using the expression

$$\begin{aligned}\langle\langle \tilde{\mathbf{F}}_\mu^{\ddagger}(\mathbf{r}) | \tilde{\mathbf{F}}_\mu(\mathbf{r}) \rangle\rangle = &\frac{1}{2\epsilon_0} \int_V \epsilon_0 \epsilon_{\mathrm{r}}(\mathbf{r}) \tilde{\mathbf{f}}_\mu(\mathbf{r}) \cdot \tilde{\mathbf{f}}_\mu(\mathbf{r}) - \mu_0 \tilde{\mathbf{g}}_\mu(\mathbf{r}) \cdot \tilde{\mathbf{g}}_\mu(\mathbf{r})\, \mathrm{d}V \\ &+ \frac{\mathrm{i}}{2\epsilon_0\tilde{\omega}_\mu} \int_{\partial V} \left[\tilde{\mathbf{f}}_\mu(\mathbf{r}) \times \left(r\partial_r \tilde{\mathbf{g}}_\mu(\mathbf{r}) \right) - \left(r\partial_r \tilde{\mathbf{f}}_\mu(\mathbf{r}) \right) \times \tilde{\mathbf{g}}_\mu(\mathbf{r}) \right] \cdot \mathbf{n}_V \, \mathrm{d}A,\end{aligned} \tag{2}$$

where $\tilde{\mathbf{F}}_\mu(\mathbf{r}) = \left[\tilde{\mathbf{f}}_\mu(\mathbf{r}), \tilde{\mathbf{g}}_\mu(\mathbf{r})\right]^{\mathrm{T}}$, in which $\tilde{\mathbf{f}}_\mu(\mathbf{r})$ and $\tilde{\mathbf{g}}_\mu(\mathbf{r})$ represent the electric and magnetic QNMs, respectively, and μ_0 denotes the vacuum permeability. The cavity is defined by the relative permittivity $\epsilon_{\mathrm{r}}(\mathbf{r})$ and we neglect magnetic material responses. V denotes the integration volume with boundary ∂V and normal vector $\mathbf{n}_V$ completely enclosing the cavity.

The electric field in the optical cavity can be decomposed in terms of the normalized QNMs as

$$\mathbf{E}(\mathbf{r})\exp(-\mathrm{i}\omega t) = \sum_\mu E_\mu(t) \tilde{\mathbf{f}}_\mu(\mathbf{r}), \tag{3}$$

where E_μ obeys a temporal coupled-mode theory (CMT) equation of the form

$$\frac{\mathrm{d}}{\mathrm{d}t} E_\mu(t) = -\mathrm{i}\tilde{\omega}_\mu E_\mu(t) - \mathrm{i}A_\mu(t), \tag{4}$$

where $A_\mu(t)$ is the coupling of the incoming field to the μ-th QNM [7].

When the sphere is hosted in the nanocavity, it gives rise to a scattered field that must be coherently added to the electric field in Eq. (1). By calculating the scattered field using the Lippmann-Schwinger equation and a QNM decomposition of the Green tensor, we find a frequency shift of the μ-th mode, which depends on the center-of-mass position of the particle, $\mathbf{r}_{\mathrm{p}}$. This eigenfrequency is denoted $\tilde{\omega}_\mu(\mathbf{r}_{\mathrm{p}}) = \tilde{\omega}_\mu + \Delta\tilde{\omega}_\mu(\mathbf{r}_{\mathrm{p}})$. Assuming the electric QNM to be constant over the sphere, we may calculate the perturbative frequency shift as,

$$\Delta\tilde{\omega}_\mu(\mathbf{r}_{\mathrm{p}}) = -\frac{\tilde{\omega}_\mu \alpha(\omega)}{2\epsilon_0 v_\mu(\mathbf{r}_{\mathrm{p}})}, \tag{5}$$

where $v_\mu(\mathbf{r}) = \langle\langle \tilde{\mathbf{F}}^{\ddagger}_\mu(\mathbf{r})|\tilde{\mathbf{F}}_\mu(\mathbf{r})\rangle\rangle/(\epsilon_{\rm r}(\mathbf{r})\tilde{\mathbf{f}}^2_\mu(\mathbf{r}))$ is the generalized mode volume from which we can define the effective mode-volume $V_{\rm eff}$ using $1/V_{\rm eff} = {\rm Re}(1/v_\mu)$ [9]. The real part of Eq. (5) represents the resonance frequency shift, whereas the imaginary part corresponds to the change in the field escape rate. Both depend on the particle location.
By letting $\tilde{\omega}_\mu \to \tilde{\omega}_\mu(\mathbf{r})$ in Eq. (4) and using the fact that the time scale of the cavity dynamics is significantly faster than the time scale of the mechanics, we may calculate the steady-state value of Eq. (4) and insert in Eq. (3). With a single-QNM approximation of the empty cavity field, which we justify in the results section, we thus finally arrive at the cycle-averaged optical force on the nanosphere

$$\begin{aligned}\langle\mathbf{F}\rangle \approx \frac{\alpha_{\rm R}}{4}|E_{\rm c}(\mathbf{r})|^2\nabla\left(\left|\tilde{\mathbf{f}}_{\rm c}\right|^2\right) + \frac{|E_{\rm c}(\mathbf{r})|^2}{\rm c}{\rm Re}\left[\tilde{\sigma}_{\rm c}(\mathbf{r})\langle\tilde{\mathbf{s}}_{\rm c}\rangle\right] + |E_{\rm c}(\mathbf{r})|^2{\rm c}\tilde{\sigma}_{\rm c}(\mathbf{r})\nabla\times\langle\tilde{\mathbf{L}}_{\rm c}\rangle \\ + \frac{\alpha_{\rm R}}{4}\left|\tilde{\mathbf{f}}_{\rm c}\right|^2\nabla\left(|E_{\rm c}(\mathbf{r})|^2\right) + {\rm c}\tilde{\sigma}(\mathbf{r})\left[\nabla(|E_{\rm c}(\mathbf{r})|^2) + E^*_{\rm c}(\mathbf{r})\nabla E_{\rm c}(\mathbf{r})\right]\times\langle\tilde{\mathbf{L}}_{\rm c}\rangle,\end{aligned} \tag{6}$$

where $E_{\rm c}(\mathbf{r}) = a_{\rm c}/[\omega_{\rm in} - (\tilde{\omega}_{\rm c} + \Delta\tilde{\omega}_{\rm c}(\mathbf{r}))]$ with $a_{\rm c} = A_{\rm c}(t)\exp({\rm i}\omega_{\rm in}t)$. Inspired by the formulation of Eq. (1), we have set $\sigma_{\rm c}(\mathbf{r}) = \alpha_{\rm I}\tilde{\omega}_{\rm c}(\mathbf{r})/{\rm c}$, $\langle\tilde{\mathbf{s}}_{\rm c}\rangle = (1/2)\tilde{\mathbf{f}}^*_{\rm c}\times\tilde{\mathbf{g}}_{\rm c}$ and $\langle\tilde{\mathbf{L}}_{\rm c}\rangle = [\epsilon_0/(4{\rm i}\tilde{\omega}_{\rm c}(\mathbf{r}))]\tilde{\mathbf{f}}_{\rm c}\times\tilde{\mathbf{f}}^*_{\rm c}$.
The first three terms in Eq. (6) correspond to the gradient force, the radiation pressure, and the spin-curl force terms. The remaining force terms in Eq. (6) are alterations to the optical force due to the position-dependent frequency perturbation and vanish in the limit of a negligible frequency perturbation.

We compare the result of the optical force modeling with reference calculations using the MST formalism. This is done by full numerical calculations of the total electromagnetic field with the sphere positioned at a particular position in the cavity and calculating the cycle-averaged force acting upon the particle as [8]

$$\langle\mathbf{F}\rangle = \int_{\partial\Omega}\langle\overleftrightarrow{\mathbf{T}}(\mathbf{r},t)\rangle\cdot\mathbf{n}_\Omega\,{\rm d}A, \tag{7}$$

where $\partial\Omega$ is a surface enclosing the particle, $\mathbf{n}_\Omega$ is the normal vector to $\partial\Omega$, and $\overleftrightarrow{\mathbf{T}}(\mathbf{r},t)$ is the Maxwell Stress tensor, given by

$$\overleftrightarrow{\mathbf{T}}(\mathbf{r},t) = \epsilon_0\mathbf{E}_{\rm tot}(\mathbf{r},t)\otimes\mathbf{E}_{\rm tot}(\mathbf{r},t) + \mu_0\mathbf{H}_{\rm tot}(\mathbf{r},t)\otimes\mathbf{H}_{\rm tot}(\mathbf{r},t) - \frac{1}{2}\left(\epsilon_0E^2_{\rm tot} + \mu_0H^2_{\rm tot}\right)\overleftrightarrow{\mathbb{1}}, \tag{8}$$

where $\otimes$ denotes the outer product, $\overleftrightarrow{\mathbb{1}}$ is the unit dyad, and $E^2_{\rm tot}$ and $H^2_{\rm tot}$ are the squared magnitudes of the total electric and magnetic fields, respectively.

Results

We base the examples in this section on the silicon nanobeam cavity from Seidler *et al.* [10], which features an effective mode-volume below the diffraction limit while maintaining a large quality factor. The large cavity Q stems from seven air holes acting as Bragg reflectors on either side of a central part with a narrow slot. The low effective mode volume stems from the nanostructuring in the center exploiting the continuity of the normal component of the displacement field, which for large permittivity discontinuities leads to a strongly confined electric field. The large ratio of $Q/V_{\rm eff}$ results in strong light-matter interaction strengths. The cavity is shown in Figure 1, where the color map shows the magnitude of the electric field solution at the center of the cavity when resonantly excited. To excite the field in Figure 1, the input field needs to be linearly polarized in y, and hence, we set $\mathbf{E}_{\rm in}(\mathbf{r}) = E_0\hat{\mathbf{e}}_ye^{-{\rm i}k_0z}$ where E_0 represents the amplitude of the field resulting in an intensity of $51.43\,\mu$W/μm^2.

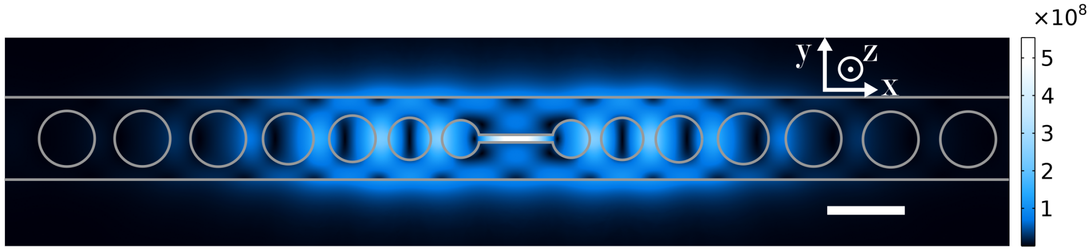

Figure 1: Design of dielectric cavity from Seidler *et al.* [10], with a total of 14 air holes. Cavity is driven on resonance, color bar is the electric-field magnitude at $z = 0$ in units of V/m. Scale bar is 500 nm, and the total length is 8.37 μm.

Before comparing the optical force modeling to reference calculations, we justify the single-mode approximation used to arrive at the result in Eq. (6). Figure 2 shows the electric-field magnitude in the center of the cavity as calculated using the single-QNM approximation along with a full numerical reference calculation. For both calculations, we use the same plane wave excitation as for Figure 1. Furthermore, the mesh and the finite element discretization is identical for the two simulations, such that any numerical error in the geometry representation is shared. We find good agreement, with relative errors below 1/1000 on resonance. A slight difference between the two calculations may be attributed to low-Q background modes. Nevertheless, the striking agreement justifies the single QNM approximation used in the force modeling in the methods section.

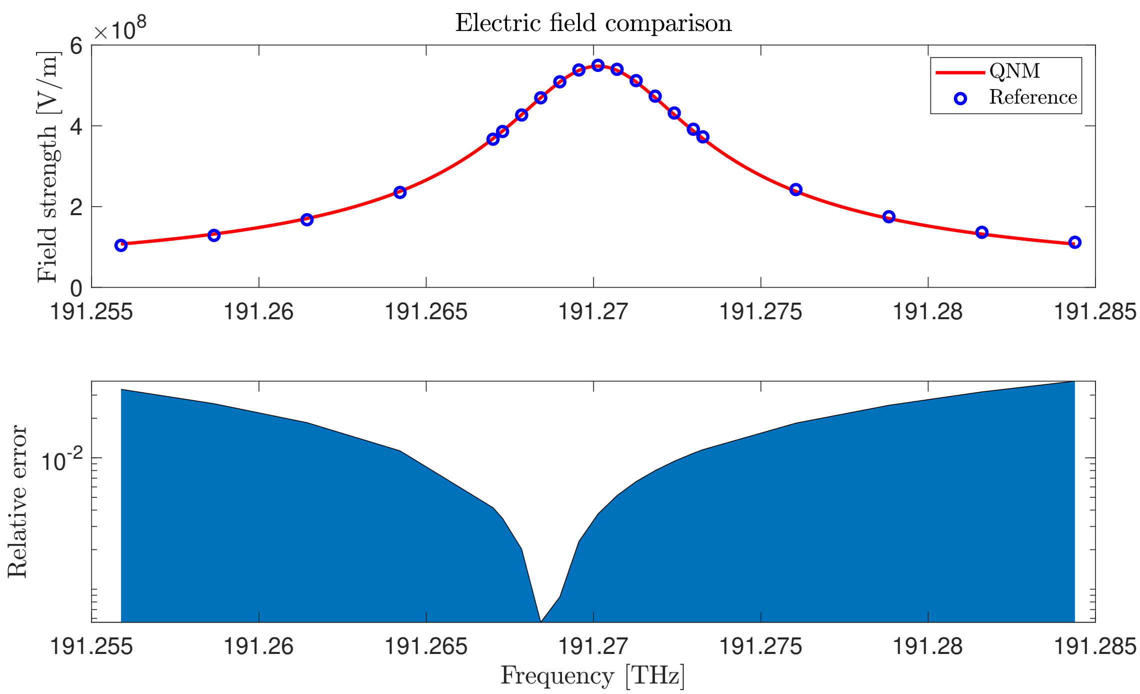

Figure 2: Comparison of single-QNM approximation for the cavity field with full numerical calculation at the center of the cavity, both calculated on an identical numerical mesh.

For small perturbations, e.g small particles or low index contrast, where $\text{Re}\left[\Delta\tilde{\omega}_c(\mathbf{r})\right]/\gamma_c \approx 0$, the optical force in Eq. (6) reduces to Eq. (1) with the field being approximated using a single-QNM approximation in Eq. (3). Similar to results from Neumeier *et al* [6], when $\text{Re}\{\Delta\tilde{\omega}_c(\mathbf{r})\}/\gamma_c \approx 1$, we observe deviations from standard dipolar force theory, and find that the force is highly dependent on the detuning of the cavity with respect to the input driving laser frequency. For lossless spheres, $\text{Im}\left[\Delta\tilde{\omega}_c(\mathbf{r})\right]$ corresponds to the increased scattering caused by the introduction of the sphere in the resonator.
To obtain the known effect of SIBA, yielding increased trap stiffness and thus further confinement, the driving frequency is redshifted such that $\omega_{\text{in}} = \text{Re}\left[\tilde{\omega}_c + \Delta\tilde{\omega}_c(\mathbf{0})\right]$. While this behavior is what we will focus on in this work, it is worth mentioning that choosing the detuning anywhere between $\text{Re}\left[\tilde{\omega}_c + \Delta\tilde{\omega}_c(\mathbf{0})\right]$ and $\text{Re}\left[\tilde{\omega}_c\right]$ enable control of the exact trapping location for the particle, and thus leads to interesting trap reconfiguration possibilities.
In Figure 3 we compare the force modeling using the frequency-perturbed QNM with a reference calculation based on the MST formalism. We choose a nanosphere of silica with a diameter of 16 nm.

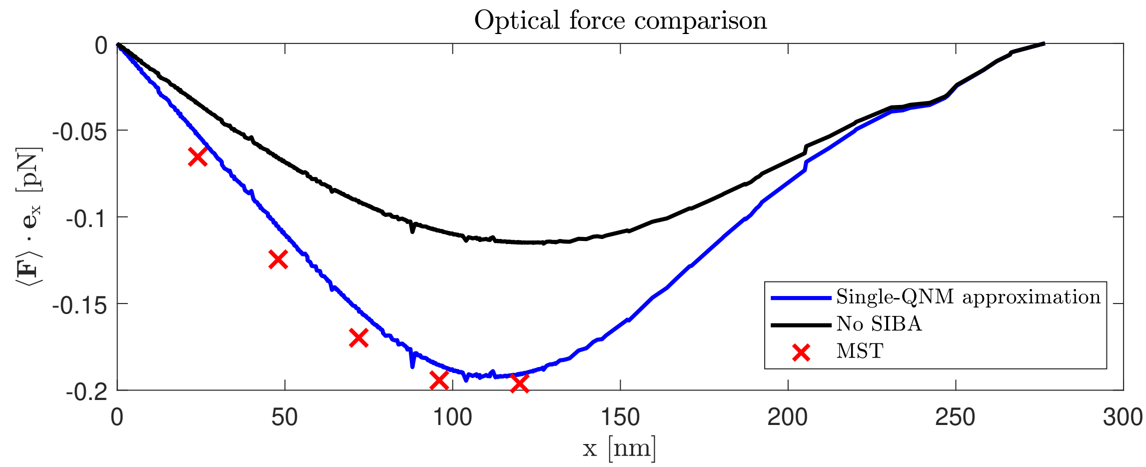

Figure 3: The x-component at $z = y = 0$ of cycle-averaged optical force using the single-QNM approximation, compared with reference calculation using MST formalism.

The empty-cavity QNM is driven with the same plane-wave illumination as the calculation based on the MST where $\omega_{\text{in}} = \text{Re}\{\tilde{\omega}_c + \Delta\tilde{\omega}_c(\mathbf{0})\}$ for both simulations. This sphere results in $\text{Re}\{\tilde{\omega}_c(\mathbf{0})\}/\gamma_c = 0.71$. The blue curve in Figure 3 represents the sum of the x-components of the force in Eq. (6) where the red crosses represent the x component of the force calculated using Eq. (8). We generally see good agreement with the MST calculation when using the frequency perturbation, suggesting that SIBA can be attributed to the frequency shift. In particular, the neglect of the frequency perturbation terms in Eq. (6) leads to significant deviations, as shown with the black curve. Interestingly, for lossless nanospheres with higher real-valued polarizabilities than used here, the deviation from the MST calculation grows. This is surprising given the accuracy of the single-QNM approximation seen in Figure 2 and suggests that the efficient modeling of optical forces with SIBA shown in this paper, while yielding good agreement for the presented particle choice, may in general have additional non-trivial corrections to the force.

Acknowledgements

We gratefully acknowledge financial support from the Danish National Research Foundation through NanoPhoton - Center for Nanophotonics, grant number DNRF147. We acknowledge SPIE for their financial conference support.

References

[1] Arthur Ashkin, J. M. Dziedzic, J E Bjorkholm, and Steven Chu. Observation of a single-beam gradient force optical trap for dielectric particles. March 1986.

[2] Yuanjie Pang and Reuven Gordon. Optical Trapping of a Single Protein. Nano Letters, 12(1):402–406, January 2012.

[3] Marcus Albrechtsen, Babak Vosoughi Lahijani, Rasmus Ellebæk Christiansen, Vy Thi Hoang Nguyen, Laura Nevenka Casses, Søren Engelberth Hansen, Nicolas Stenger, Ole Sigmund, Henri Jansen, Jesper Mørk, and Søren Stobbe. Nanometer-scale photon confinement in topology-optimized dielectric cavities. Nature Communications, 13(1):6281, October 2022.

[4] Nicolas Descharmes, Ulagalandha Perumal Dharanipathy, Zhaolu Diao, Mario Tonin, and Romuald Houdré. Observation of Backaction and Self-Induced Trapping in a Planar Hollow Photonic Crystal Cavity. Physical Review Letters, 110(12):123601, March 2013.

[5] Donato Conteduca, Giuseppe Brunetti, Giampaolo Pitruzzello, Francesco Tragni, Kishan Dholakia, Thomas F. Krauss, and Caterina Ciminelli. Exploring the Limit of Multiplexed Near-Field Optical Trapping. ACS Photonics, 8(7):2060–2066, July 2021.

[6] Lukas Neumeier, Romain Quidant, and Darrick E Chang. Self-induced back-action optical trapping in nanophotonic systems. New Journal of Physics, 17(12):123008, December 2015.

[7] Philip Trøst Kristensen, Kathrin Herrmann, Francesco Intravaia, and Kurt Busch. Modeling electromagnetic resonators using quasinormal modes. Advances in Optics and Photonics, 12(3):612, September 2020.

[8] Lukas Novotny and Bert Hecht. Principles of Nano-Optics. Cambridge University Press, Cambridge, 2 edition, 2012.

[9] P. T. Kristensen, C. Van Vlack, and S. Hughes. Generalized effective mode volume for leaky optical cavities. Optics Letters, 37(10):1649–1651, May 2012. Publisher: Optica Publishing Group.

[10] Paul Seidler, Kevin Lister, Ute Drechsler, Jens Hofrichter, and Thilo Stöferle. Slotted photonic crystal nanobeam cavity with an ultrahigh quality factor-to-mode volume ratio. Optics Express, 21(26):32468–32483, December 2013. Publisher: Optica Publishing Group.